Innermost stable circular orbit of a spinning particle in Kerr spacetime

Shingo Suzuki* and Kei-ichi Maeda†
Department of Physics, Waseda University, Shinjuku-ku, Tokyo 169, Japan
(Received 29 December 1997; published 25 June 1998)

We study the stability of circular orbits of spinning test particles in Kerr spacetime. We find that some of the circular orbits become unstable in the direction perpendicular to the equatorial plane, although the orbits are still stable in the radial direction. For the large spin case [$\mathcal{S}/\mu M \lesssim O(1)$], the innermost stable circular orbit (ISCO) appears before the minimum of the effective potential in the equatorial plane disappears. This changes the radius of the ISCO and therefore the frequency of the last circular orbit. [S0556-2821(98)04014-4]

PACS number(s): 97.80.−d, 04.25.−g, 04.70.Bw

I. INTRODUCTION

Coalescence of two compact objects, such as neutron-star–neutron-star, neutron-star–black-hole, and/or black-hole–black-hole binaries, is one of the promising sources of gravitational waves which may be detected in the near future by laser interferometric detectors, such as the U.S. Laser Interferometric Gravitational Wave Observatory (LIGO) [1]. If we detect a signal of gravitational waves emitted from those systems and compare it with theoretical templates, we may be able not only to determine a variety of astrophysical parameters of the sources, e.g., their orbital information, masses, and spins, but also to obtain more information about fundamental physics, e.g., the equation of state at high density [2]. In order to obtain such important information from the observed data, we have to make an exact template and then we need to know the exact motion of the binary. Hence the equations of motion in the post-Newtonian framework have been studied by many authors [3]. We can see from the obtained equations of motion that spins of stars play a very important role. For example, this effect induces a precession of the orbital plane, resulting in modulation of the gravitational wave forms [4]. Although such post-Newtonian approaches are definitely important, a fully general relativistic treatment must become necessary at some stage. Numerical relativity is one of most promising treatments to give a correct template, but it is still at a developing stage. Instead, the black hole perturbation technique has been well studied and provides us a good approximation. We expect that the general relativistic spin effect is also well understood by such a perturbation approach.

Many studies about a relativistic spin effect using a spinning test particle around a black hole have been made since the basic equations were first derived by Papapetrou [5] and reformulated by Dixon [6]. Bailey and Israel elaborated this system using the Lagrangian formalism [7]. Corinaldesi and Papapetrou first discussed the motion of a spinning test particle in Schwarzschild spacetime [8]. The Kerr or Kerr-Newman spacetime case was also analyzed by several authors [9]. In [10], the gravitational waves produced by a spinning particle falling into a Kerr black hole or moving circularly around it were discussed and the energy emission rate from those systems was calculated. We investigated more generic motion of a spinning particle around a Schwarzschild black hole and pointed out that the spin effect can make some orbits chaotic [11].

When we discuss the gravitational waves from a binary system, one of the most important keys is the innermost stable circular orbit (ISCO). In the binary system, as gravitational waves are emitted, both energy and angular momentum of the system decrease, and so the orbital radius gradually decreases. When the angular momentum is reduced below some critical value, we cannot find any circular orbit. The binary system evolves from the quasi-stationary stage into a more dynamical stage, i.e., the stars in the system collide with each other. The last circular orbit is the ISCO. It may determine the observable frequency of the system. Using the effective potential of the spinning particle in the equatorial plane, the binding energy of the circular orbit is discussed in [9]. They assumed that a stable circular orbit exists unless the minimum point of the effective potential in the equatorial plane disappears.

However, before the system reaches such a last orbit, if there exists any unstable mode, it will change the ISCO, and therefore the last circular radius, binding energy and frequency, which may be important in gravitational wave astronomy. In [9], the instability of a circular orbit in the radial direction is discussed. In [11], we found that some circular orbits of a spinning particle in Schwarzschild spacetime become unstable in the direction perpendicular to the equatorial plane [11].

In this paper, extending our previous analysis [11], we study an instability of the spinning test particle in a Kerr spacetime. There are three reasons for a transition from the quasi-periodic stage to dynamical stage. The most important one is general relativistic strong gravity, i.e., when the orbital separation of the binary becomes small as $r \sim 6M$, the centrifugal force cannot be balanced with the gravitational force, so that the star cannot stop from changing its circular orbit to a plunging one. The second effect is the hydrodynamical interaction between two stars, i.e., at the moment when the surfaces of the stars come into contact, we expect that such a transition will occur due to the direct interaction between stars. The third one is an effect due to an intrinsic property of the star such as a mass quadrupole moment. For example, in [12], they show that instability can occur due to a tidal force. When the orbital separation of the stars becomes small, each star of the binary is significantly deformed by a tidal force.

*Electronic address: shingo@gravity.phys.waseda.ac.jp
†Electronic address: maeda@mse.waseda.ac.jp

As a result, circular orbits of the stars become unstable and the ISCO appears earlier. In this analysis, however, the motion of the stars is restricted to the equatorial plane and the stars plunge into each other when the motion becomes unstable in the radial direction. Here, we look for a new type of instability due to an effect belonging to the third category, i.e., the instability in the direction perpendicular to the equatorial plane. We will show that such an instability really occurs when the spin of a test particle is high. A spinning particle leaves the equatorial plane and falls into black hole. Since it is important to determine the ISCO for gravitational wave astronomy, we believe that it is also worthwhile to analyze such a new instability of a spinning particle in Kerr spacetime.

This paper is organized as follows. After a brief review of the basic equations in Sec. II, we analyze the stability of a circular orbit of a spinning test particle in Sec. III, using a linear perturbation method. We show changes of the radius of the ISCO, of the binding energy and of the frequency due to such an instability. A summary and some remarks follow in Sec. IV. Throughout this paper we use units $c=G=1$. Our notation including the signature of the metric follows that of Misner, Thorne, and Wheeler (MTW) [13].

II. BASIC EQUATIONS FOR A SPINNING TEST PARTICLE

A. Pole-dipole approximation

The equations of motion of a spinning test particle in a relativistic spacetime were first derived by Papapetrou [5] and then reformulated by Dixon [6]. These are a set of equations:

$$\frac{dx^\mu}{ds}=v^\mu, \tag{2.1}$$

$$\frac{Dp^\mu}{ds}=-\frac{1}{2}R^\mu{}_{\nu\rho\sigma}v^\nu S^{\rho\sigma}, \tag{2.2}$$

$$\frac{DS^{\mu\nu}}{ds}=p^\mu v^\nu-p^\nu v^\mu, \tag{2.3}$$

where s, v^μ, p^μ and $S^{\mu\nu}$ are an affine parameter of the orbit $x^\mu=x^\mu(s)$, the 4-velocity of the particle, the momentum, and the spin tensor, respectively. This is called the pole-dipole approximation, where the multipole moments of the particle higher than mass monopole and spin dipole are ignored. We need a supplementary condition which gives a relation between v^μ and p^μ, because p^μ is no longer parallel to v^μ. The consistent choice of the center of mass provides such a condition [6]:

$$p_\mu S^{\mu\nu}=0. \tag{2.4}$$

Using Eq. (2.4) we find the relation between v^μ and p^μ as

$$v^\mu=N\left[u^\mu+\frac{1}{2\mu^2\delta}S^{\mu\nu}u^\lambda R_{\nu\lambda\rho\sigma}S^{\rho\sigma}\right], \tag{2.5}$$

where

$$\delta=1+\frac{1}{4\mu^2}R_{\alpha\beta\gamma\delta}S^{\alpha\beta}S^{\gamma\delta}, \tag{2.6}$$

and N is a normalization constant, which is fixed by a choice of the affine parameter s. $u^\nu\equiv p^\nu/\mu$ is a normalized momentum, where the mass of the particle μ is defined by

$$\mu^2=-p_\nu p^\nu. \tag{2.7}$$

It may sometimes be more convenient or more intuitive to describe the basic equations by use of a spin vector S_μ, which is defined by

$$S_\mu=-\frac{1}{2}\epsilon_{\mu\nu\rho\sigma}u^\nu S^{\rho\sigma}, \tag{2.8}$$

where $\epsilon^{\mu\nu\rho\sigma}$ is the Levi-Civita tensor. The basic equations are now

$$\frac{dx^\mu}{ds}=v^\mu, \tag{2.9}$$

$$\frac{Dp^\mu}{ds}=\frac{1}{\mu}R^*{}^\mu{}_{\nu\rho\sigma}v^\nu S^\rho p^\sigma, \tag{2.10}$$

$$\frac{DS^\mu}{ds}=\frac{1}{\mu^3}p^\mu R^*{}_{\nu\lambda\rho\sigma}S^\nu v^\lambda S^\rho p^\sigma, \tag{2.11}$$

where

$$R^*{}_{\mu\nu\rho\sigma}\equiv\frac{1}{2}R_{\mu\nu}{}^{\alpha\beta}\epsilon_{\alpha\beta\rho\sigma}. \tag{2.12}$$

Equation (2.4) with the definition (2.8) reads

$$p_\nu S^\nu=0, \tag{2.13}$$

which gives the relation between v^μ and p^μ,

$$v^\mu=u^\mu+\frac{1}{\mu^2}\,{}^*R^*{}^\mu{}_{\nu\rho\sigma}S^\nu S^\rho u^\sigma, \tag{2.14}$$

where

$${}^*R^*{}_{\mu\nu\rho\sigma}\equiv\frac{1}{2}\epsilon_{\mu\nu\alpha\beta}R^*{}^{\alpha\beta}{}_{\rho\sigma}; \tag{2.15}$$

we fix the affine parameter s using the condition $v^\mu u_\mu=-\delta$. This choice makes the perturbation equations simpler as we will show later.

For a particle motion in a Kerr spacetime, we find several conserved quantities. Regardless of the symmetry of the background spacetime, it is easy to show that μ and the magnitude of spin $\mathcal{S}$, defined by

$$\mathcal{S}^2\equiv S_\nu S^\nu, \tag{2.16}$$

are constants of motion. When the spacetime possesses some symmetry described by a Killing vector ξ^μ,

$$C\equiv\xi^\mu p_\mu-\frac{1}{2}\xi_{\mu;\nu}S^{\mu\nu} \tag{2.17}$$

is conserved [6]. For the spacetime which has both axial and timelike Killing vectors such as Kerr spacetime, we have two

conserved quantities, i.e., the energy E and the z component of the total angular momentum of a spinning particle J_z. For Schwarzschild spacetime, the ''x'' and ''y'' components of the total angular momentum of a particle are also conserved because of spherical symmetry.

B. Effective potential of a spinning particle on the equatorial plane

In order to discuss the motion of a test particle in a black hole spacetime, we usually introduce an effective potential. However, if the test particle has a spin, it is not so easy to find an effective potential because of an additional dynamical freedom of the spin direction. In our previous paper, we defined an ''effective potential'' for a spinning test particle in Schwarzschild spacetime, i.e., $V_{(\pm)}(r,\theta;J,\mathcal{S})$ given by Eqs. (2.31) and (2.32) in [11]. Setting the total angular momentum so as to point in the z direction, i.e., $(J_x,J_y,J_z)=(0,0,J)$, those equations are obtained from the condition of $p^r=p^\theta=0$ in Eqs. (2.4) and (2.7). We use quotation marks because it is not a real effective potential but plays a similar role.

The particle with energy E can move within the contour curve defined by

$$E=V_{(\pm)}(r,\theta;J,\mathcal{S}). \tag{2.18}$$

This ''effective potential'' has two parameters, J and $\mathcal{S}$, whose values determine the topology of its contours. From the contours of the ''effective potential'' (Fig. 2 in [11]), we can easily see the stability of a bound orbit.

However, since we are interested in a Kerr background spacetime, whose metric is given as

$$ds^2=-\left(1-\frac{2Mr}{\Sigma}\right)dt^2+\frac{\Sigma}{\Delta}dr^2+\Sigma d\theta^2 + \frac{\mathcal{A}}{\Sigma}\sin^2\theta d\phi^2-\frac{4Ma}{\Sigma}r\sin^2\theta dt d\phi, \tag{2.19}$$

where

$$\Sigma=r^2+a^2\cos^2\theta,\quad \Delta=r^2-2Mr+a^2, \quad \mathcal{A}=(r^2+a^2)^2-a^2\Delta\sin^2\theta, \tag{2.20}$$

it is hard to define an effective potential even in the above naive sense. This is because we cannot find new conserved quantities in a Kerr background spacetime, which correspond to J_x, J_y for the Schwarzschild case or Carter's constant for a spinless particle [13], in addition to E and J_z. However, if we restrict the particle motion to the equatorial plane, an effective potential for the radial motion is found [9]. The direction of spin must be parallel to the rotational axis. In fact, imposing $\theta=\pi/2$, $S^0=S^1=S^3=0$, $S^2\equiv-\mathcal{S}$ and $p^2=0$ to Eq. (2.17), we find that the energy and the z component of the angular momentum take the following forms:

$$-E=\frac{\sqrt{\Delta}}{r}p_0-\frac{1}{r}\left(a+\frac{M\mathcal{S}}{\mu r}\right)p_3, \tag{2.21}$$

$$J_z=-\frac{\sqrt{\Delta}}{r}\left(a+\frac{\mathcal{S}}{\mu}\right)p_0+\frac{1}{r}\left[r^2+a^2+\frac{a\mathcal{S}(r+M)}{\mu r}\right]p_3. \tag{2.22}$$

Solving these equations with respect to p_0 and p_3 and using the solutions and $p_2=0$, we find that Eq. (2.7) is reduced to

$$(p_1)^2=A(E-U_{(+)})(E-U_{(-)}), \tag{2.23}$$

and

$$U_{(\pm)}(r;J_z,\mathcal{S},a)=XJ_z\pm\sqrt{(X^2-Y)J_z^2-Z}, \tag{2.24}$$

$$X=\frac{\left[r^2+a^2+\frac{a\mathcal{S}}{\mu}\left(1+\frac{M}{r}\right)\right]\left(a+\frac{M\mathcal{S}}{\mu r}\right)-\Delta\left(a+\frac{\mathcal{S}}{\mu}\right)}{\left[r^2+a^2+\frac{a\mathcal{S}}{\mu}\left(1+\frac{M}{r}\right)\right]^2-\Delta\left(a+\frac{S}{\mu}\right)^2},$$

$$Y=\frac{\left(a+\frac{M\mathcal{S}}{\mu r}\right)^2-\Delta}{\left[r^2+a^2+\frac{a\mathcal{S}}{\mu}\left(1+\frac{M}{r}\right)\right]^2-\Delta\left(a+\frac{\mathcal{S}}{\mu}\right)^2},$$

$$Z=-\frac{\Delta\left(\frac{M\mathcal{S}^2}{\mu^2r^2}-r\right)\mu^2}{\left[r^2+a^2+\frac{a\mathcal{S}}{\mu}\left(1+\frac{M}{r}\right)\right]^2-\Delta\left(a+\frac{\mathcal{S}}{\mu}\right)^2},$$

$$A=\frac{\left[r^2+a^2+\frac{a\mathcal{S}}{\mu}\left(a+\frac{M}{r}\right)\right]^2-\Delta\left(a+\frac{\mathcal{S}}{\mu}\right)^2}{\Delta\left(\frac{M\mathcal{S}^2}{\mu^2r^2}-r\right)^2}.$$

Note that the suffices of the momentum and the spin vector denote tetrad components. The tetrad frame has been defined as

$$\begin{aligned} e^0_\mu&=\left(\sqrt{\frac{\Delta}{\Sigma}},0,0,-a\sin^2\theta\sqrt{\frac{\Delta}{\Sigma}}\right),\\ e^1_\mu&=\left(0,\sqrt{\frac{\Sigma}{\Delta}},0,0\right),\\ e^2_\mu&=(0,0,\sqrt{\Sigma},0),\\ e^3_\mu&=\left(-\frac{a}{\sqrt{\Sigma}}\sin\theta,0,0,\frac{r^2+a^2}{\sqrt{\Sigma}}\sin\theta\right), \end{aligned} \tag{2.25}$$

where $e^i_\mu=(e^i_t,e^i_r,e^i_\theta,e^i_\phi)$ for $i=0\sim3$. $\mathcal{S}$ includes the direction of spin as well as the magnitude. Then $a\mathcal{S}>0$ means the spin of the particle is parallel to that of the black hole and $a\mathcal{S}<0$ means anti-parallel.

We regard $U_{(\pm)}(r;J_z,\mathcal{S},a)$ as an effective potential of the particle on the equatorial plane. When a vanishes, $U_{(+)}$ is reduced to $V_{(-)}(r,\pi/2;J,\mathcal{S})$ in the Schwarzschild case [11] for $\mathcal{S}J_z>0$ and to $V_{(+)}(r,\pi/2;J,\mathcal{S})$ for $\mathcal{S}J_z<0$. The particle with energy E can move only in the region of $E\geqslant U_{(+)}$ (or $E\leqslant U_{(-)}$) on the equatorial plane. The typical shape of $U_{(\pm)}$ is shown in Fig. 1. We usually discuss the orbit in the equa-

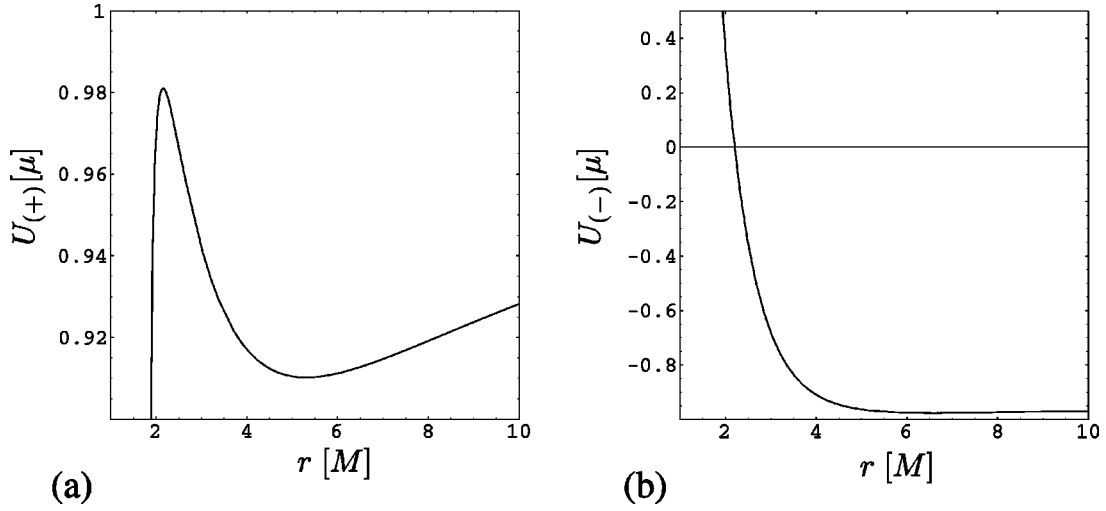

FIG. 1. The effective potential $U_{(\pm)}$ on the equatorial plane for $J_z=4\mu M$, $\mathcal{S}=1\mu M$ and $a=0.5M$. (a) The potential $U_{(+)}$ has two extremal points. (b) The potential $U_{(-)}$ has no extremum. A particle with positive energy is not bounded.

torial plane by use of this effective potential. In the case of a spinless particle, it is enough because the conservation of angular momentum prevents the particle from leaving the equatorial plane. If the angular momentum is larger than some critical value, we always find a stable circular orbit. Since no circular orbit exists below the critical angular momentum, the particle eventually enters a dynamical stage from a quasi-periodic stage because the emitted gravitational waves remove angular momentum from the system. This critical value gives the ISCO. If a test particle has a spin, however, the orbital angular momentum need not be conserved. The particle may move off the equatorial plane. Hence the analysis by use of the above effective potential may not give the ISCO. We need a more detailed analysis to see whether the circular orbit on the equatorial plane is really stable or not.

III. STABILITY OF A CIRCULAR ORBIT OF A SPINNING PARTICLE

The linear perturbation method is used to analyze the stability of a circular orbit of a spinning particle. In the tetrad frame, the equations of motion of a spinning particle are rewritten as

$$\frac{dx^\mu}{ds}=e^\mu_a v^a, \tag{3.1}$$

$$\frac{dp^a}{ds}=\omega_{cb}{}^a v^c p^b+\frac{1}{\mu}R^*{}^a{}_{bcd}v^b S^c p^d, \tag{3.2}$$

$$\frac{dS^a}{ds}=\omega_{cb}{}^a v^c S^b+\frac{1}{\mu^3}p^a S^i R^*{}_{ijkl}v^j S^k p^l, \tag{3.3}$$

where ω_{ijk} are the Ricci rotation coefficients defined as

$$\omega_{ijk}=e^\nu_i e^\mu_j e_{k\mu;\nu}. \tag{3.4}$$

We assume a circular orbit in the equatorial plane as an unperturbed orbit, i.e., $r_{(0)}=r_0=\text{const}$, $\theta_{(0)}=\pi/2$, $p^1_{(0)}=p^2_{(0)}=0$, $S^0_{(0)}=S^1_{(0)}=S^3_{(0)}=0$, $S^2_{(0)}=-\mathcal{S}$ and the time derivatives of these variables vanish. Here, we use the suffix (0) for the unperturbed variables. From Eq. (2.14), we find

$$v^0_{(0)}=\frac{p^0_{(0)}}{\mu}\left(1-\frac{M\mathcal{S}^2}{\mu^2 r^3}\right), \tag{3.5}$$

$$v^3_{(0)}=\frac{p^3_{(0)}}{\mu}\left(1+\frac{2M\mathcal{S}^2}{\mu^2 r^3}\right), \tag{3.6}$$

and $v^1_{(0)}=v^2_{(0)}=0$. The conserved quantities in our system are the energy and the z component of total angular momentum, which are now given as

$$E=\frac{\sqrt{\Delta}}{r_0}p^0_{(0)}+\frac{1}{r_0}\left(a+\frac{M\mathcal{S}}{\mu}\right)p^3_{(0)}, \tag{3.7}$$

$$J_z=\frac{\sqrt{\Delta}}{r_0}\left(a+\frac{\mathcal{S}}{\mu}\right)p^0_{(0)}+\frac{1}{r_0}\left[r_0^2+a^2+\frac{a\mathcal{S}}{\mu}\left(1+\frac{M}{r_0}\right)\right]p^3_{(0)}. \tag{3.8}$$

The way to determine the unperturbed variables is as follows. First, the Kerr parameter a and the magnitude of the spin $\mathcal{S}$ are fixed. Next, we give the radius of a circular orbit r_0. Then, from the condition of potential extremum at r_0, i.e.

$$\left.\frac{dU_{(+)}(r)}{dr}\right|_{r=r_0}=0, \tag{3.9}$$

J_z is determined. The energy of the particle is obtained by $E=U_{(+)}(r_0)$. Finally, from Eqs. (3.7) and (3.8), $p^0_{(0)}$ and $p^3_{(0)}$ are determined. We denote these unperturbed variables as $x^\mu_{(0)}$, $v^i_{(0)}$, $p^i_{(0)}$ and $S^i_{(0)}$. Of course, if no real solution J_z is found for given parameters a and $\mathcal{S}$, a circular orbit does not exist at r_0.

Let δx^μ, δv^i, δp^i and δS^i be the perturbations around the unperturbed variables. We shall introduce a tetrad description for δx^μ as $\delta x^i\equiv e^i_\mu \delta x^\mu$. From Eq. (2.14),

$$\delta v^i = X^i_j \delta x^j + Y^i_j \delta p^j + Z^i_j \delta S^j, \tag{3.10}$$

where,

$$X^i_j = \frac{1}{\mu} e^\mu_j \frac{\partial}{\partial x^\mu} {}^*R^{*\ i}_{(0)\ lmn} S^l_{(0)} S^m_{(0)} p^n_{(0)}, \tag{3.11}$$

$$Y^i_j = \frac{1}{\mu} \delta^i_j + \frac{1}{\mu^3} {}^*R^{*\ i}_{(0)\ lmn} S^l_{(0)} S^m_{(0)} \delta^n_j, \tag{3.12}$$

$$Z^i_j = \frac{1}{\mu^3} {}^*R^{*\ i}_{(0)\ lmn} (\delta^l_j S^m_{(0)} + S^l_{(0)} \delta^m_j) p^n_{(0)}. \tag{3.13}$$

Inserting

$$\begin{aligned} x^\mu &= x^\mu_{(0)} + e^\mu_i \delta x^i, \\ v^i &= v^i_{(0)} + \delta v^i, \\ p^i &= p^i_{(0)} + \delta p^i, \\ S^i &= S^i_{(0)} + \delta S^i, \end{aligned} \tag{3.14}$$

into Eqs. (3.1)–(3.3) and neglecting terms higher than the first order of perturbed variables, we find the linear perturbation equations as

$$\frac{d}{ds} \begin{pmatrix} \delta x^i \\ \delta p^i \\ \delta S^i \end{pmatrix} = \begin{pmatrix} A^i_j & B^i_j & C^i_j \\ D^i_j & E^i_j & F^i_j \\ G^i_j & H^i_j & I^i_j \end{pmatrix} \begin{pmatrix} \delta x^j \\ \delta p^j \\ \delta S^j \end{pmatrix}, \tag{3.15}$$

where

$$\begin{aligned} A^i_j &= X^i_j + \omega_{(0)lk}{}^i \delta^k_j v^l_{(0)} - \omega_{(0)lk}{}^i v^k_{(0)} \delta^l_j, \\ B^i_j &= Y^i_j, \\ C^i_j &= Z^i_j, \\ D^i_j &= e^\mu_j \frac{\partial}{\partial x^\mu} \omega_{(0)lk}{}^i v^l_{(0)} p^k_{(0)} + \omega_{(0)lk}{}^i X^l_j p^k_{(0)} + \Phi^i_j, \\ E^i_j &= \omega_{(0)lk}{}^i v^l_{(0)} \delta^k_j + \omega_{(0)lk}{}^i Y^l_j p^k_{(0)} + \Pi^i_j, \\ F^i_j &= \omega_{(0)lk}{}^i Z^l_j p^k_{(0)} + \Psi^i_j, \\ G^i_j &= e^\mu_j \frac{\partial}{\partial x^\mu} \omega_{(0)lk}{}^i v^l_{(0)} S^k_{(0)} + \omega_{(0)lk}{}^i X^l_j S^k_{(0)} \\ &\quad + \frac{1}{\mu^2} p^i_{(0)} S_{(0)l} \Phi^l_j, \\ H^i_j &= \frac{1}{\mu^3} R^*_{(0)abcd} S^a_{(0)} v^b_{(0)} S^c_{(0)} p^d_{(0)} \delta^i_j \\ &\quad + \omega_{(0)lk}{}^i Y^l_j S^k_{(0)} + \frac{1}{\mu^2} p^i S_{(0)l} \Pi^l_j, \\ I^i_j &= \omega_{(0)lj}{}^i v^l_{(0)} + \frac{1}{\mu^3} p^i_{(0)} R^*_{(0)jabc} v^a_{(0)} S^b_{(0)} p^c_{(0)} \\ &\quad + \omega_{(0)lk}{}^i Z^l_j S^k_{(0)} + \frac{1}{\mu^2} p^i_{(0)} S_{(0)l} \Psi^l_j, \end{aligned} \tag{3.16}$$

with

$$\begin{aligned} \Phi^i_j &= \frac{1}{\mu} \left(e^\mu_j \frac{\partial}{\partial x^\mu} R^{*\ i}_{(0)\ lmn} v^l_{(0)} + R^{*\ i}_{(0)\ lmn} X^l_j \right) S^m_{(0)} p^n_{(0)}, \\ \Pi^i_j &= \frac{1}{\mu} R^{*\ i}_{(0)\ lmn} (Y^l_j p^n_{(0)} + v^l_{(0)} \delta^n_j) S^m_{(0)}, \\ \Psi^i_j &= \frac{1}{\mu} R^{*\ i}_{(0)\ lmn} (Z^l_j S^m_{(0)} + v^l_{(0)} \delta^m_j) p^n_{(0)}. \end{aligned} \tag{3.17}$$

In the case of a spinless particle, Eq. (3.15) is nothing but the equation of geodesic deviation. The eigenvalues of the matrix in Eq. (3.15) determine the stability of a test particle. Inserting the unperturbed variables into the matrix in Eq. (3.15), the matrix becomes rather simple. In the Appendix, we show the explicit form of the matrix and its components and discuss the structure of the matrix. The eigenvalue equation forms

$$\lambda^6 (\lambda^2 - \Lambda_r)(\lambda^4 - \Lambda_{\theta 1} \lambda^2 + \Lambda_{\theta 2}) = 0, \tag{3.18}$$

where Λ_r, $\Lambda_{\theta 1}$ and $\Lambda_{\theta 2}$ are defined in the Appendix. First, to see the meaning of this equation, we consider a simple case. When $\mathcal{S}=0$ and $a=0$, this equation is reduced to

$$\lambda^8 \left(\lambda^2 + \frac{M\mu^2 (r_0 - 6M)}{r_0^3 (r_0 - 3M)} \right) \left(\lambda^2 + \frac{L_z^2}{r_0^4} \right) = 0, \tag{3.19}$$

i.e.,

$$\begin{aligned} \Lambda_r &= -\frac{M\mu^2 (r_0 - 6M)}{r_0^3 (r_0 - 3M)}, \\ \Lambda_{\theta 1} &= -\frac{L_z^2}{r_0^4}, \\ \Lambda_{\theta 2} &= 0, \end{aligned} \tag{3.20}$$

where L_z is the z component of orbital angular momentum, and it is given for an unperturbed circular orbit as

$$L_z^2 = \frac{M\mu^2 r_0^2}{r_0 - 3M}. \tag{3.21}$$

This equation shows that no circular orbit exists for $r_0 < 3M$. The positivity of the second parenthesis of Eq. (3.19) guarantees the stability in the θ direction, i.e., in the direction perpendicular to the equatorial plane. Therefore, the orbit of a spinless particle in Schwarzschild spacetime is stable against perturbations in the θ direction. The first parenthesis in Eq. (3.19) shows the stability in the r direction. For $r_0 \leqslant 6M$, the eigenvalues are real, while for $r > 6M$, those are purely imaginary. This means that the equilibrium point (circular orbit) with $r_0 \leqslant 6M$ is unstable, while it is stable for the case of $r_0 > 6M$. We find the critical radius $r = 6M$ when $L_z = \sqrt{12}\mu M$. This corresponds to the ISCO of a spinless particle in Schwarzschild spacetime.

In the general case, we can analyze the stability of the circular orbit in the r direction by Λ_r and in the θ direction by $\Lambda_{\theta 1}$ and $\Lambda_{\theta 2}$ (see also the Appendix). If $\Lambda_r > 0$, the cir-

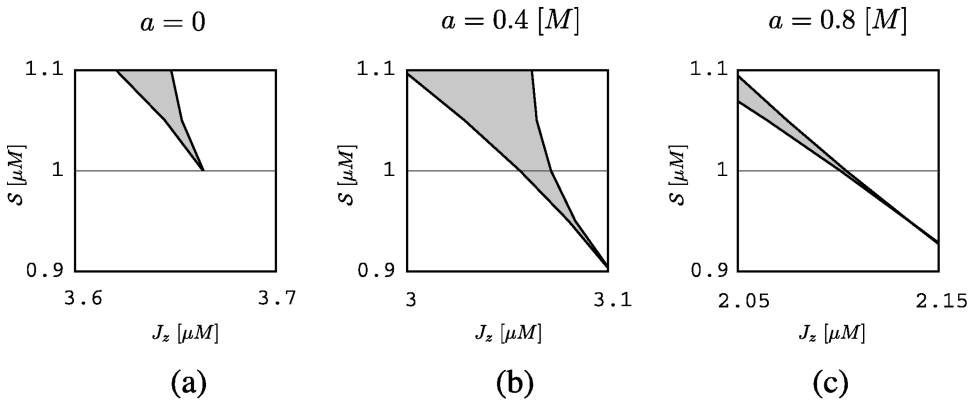

FIG. 2. The parameter regions for which the circular orbit becomes unstable in the direction perpendicular to the equatorial plane. The minimal values of the spin for each case are (a) $\mathcal{S}=0.98\mu M$, (b) $\mathcal{S}=0.9\mu M$, and (c) $\mathcal{S}=0.94\mu M$.

cular orbit is unstable against a radial perturbation, while if the real part of any solution of the equation

$$\lambda^4-\Lambda_{\theta 1}\lambda^2+\Lambda_{\theta 2}=0, \tag{3.22}$$

is positive, it is unstable against perturbations perpendicular to the equatorial plane.

In Fig. 2, we show the unstable parameter ranges by shaded regions for the case of $a=0,0.4M$ and $0.8M$. We find that the unstable parameter range is usually narrow, because we have a constraint for the particle spin as $\mathcal{S}/\mu M \lesssim O(1)$ (see the discussion in [11]). As we can see from this figure, the unstable region in the $a=0.4M$ case is larger than that in the $a=0$ case. The value of $\mathcal{S}$ at the bottom edge of this region is $\sim 0.9\mu M$. However, in the $a=0.8M$ case, the unstable region becomes narrow again. The lowest value of $\mathcal{S}$ for this region is about $0.94\mu M$.

The solid lines in Fig. 3 show the radius of the ISCO for three values of a. The radius of the ISCO decreases as $\mathcal{S}$ increases or as a increases, which means that the spin effect plays the role of a repulsive force for $a\mathcal{S}>0$ basically. Therefore, the particle can approach the horizon of the black hole without passing the horizon. But, if $\mathcal{S}$ is larger than the critical value, the radius of the ISCO increases. This shows the occurrence of the instability of the motion in the θ direction. The hatched regions below the solid lines denote the interval of radii over which an orbit is stable on the equatorial plane but unstable perpendicularly. When $S=1\mu M$, the intervals are $3.8073M \leqslant r \leqslant 3.8508M$ for $a=0$, $2.8835M \leqslant r \leqslant 3.0945M$ for $a=0.4M$ and $1.9340M \leqslant r \leqslant 1.9700M$ for $a=0.8M$, respectively. In Fig. 4, we show the energy of the particle and the orbital frequency of the ISCO. In [9], the energy the ISCO for same system was analyzed, but only the instability in the radial direction was taken into account. When the instability in the θ direction is included, the energy and frequency of the ISCO behaves in the different manner beyond the critical value.

IV. DISCUSSIONS AND SUMMARY

In our previous paper [11], we discussed the motion of a spinning test particle in a Schwarzschild spacetime by use of an ''effective potential.'' The ''effective potential'' is classified into four types depending on its topology of contour (Figs. 2 and 3 in [11]). From Fig. 2 in [11], we can see easily the stability of the circular orbit of the spinning particle in Schwarzschild background spacetime. The type(B1) has one saddle point and one minimal point on the equatorial plane. The saddle point is maximal in the r direction and minimal in the θ direction. At the minimal point, it is minimal in both directions. For the type(B2) potential, there are two saddle points away from the equatorial plane and one maximal and one minimal point also exist on the equatorial plane. In the type(U2) potential, we find one unstable point in both directions and one saddle point. At this saddle point, we find that the orbit is stable in the r direction but unstable in the θ direction. This is exactly the same as what we found in this paper as the new type of instability. The stability of the circular orbit on the equatorial plane is summarized in Table I.

For a Kerr background spacetime, however, we cannot define the effective potential for a spinning particle. Thereupon, instead of the topology of the contour, we divided the parameter space using the stability of the circular orbit. The

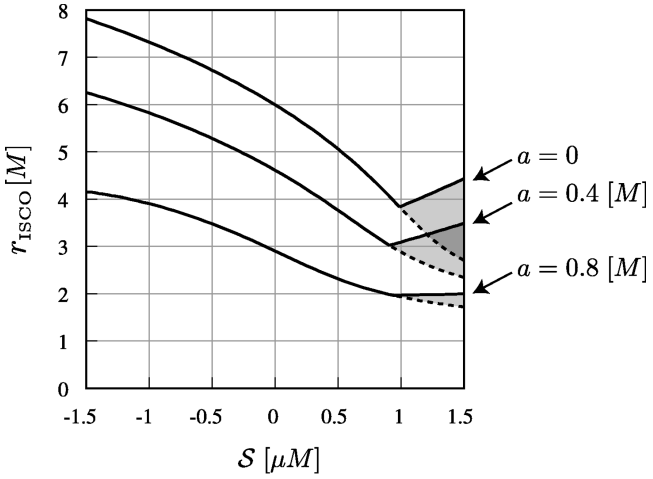

FIG. 3. The solid lines show the radius of the innermost stable circular orbit (ISCO). Above the critical value of $\mathcal{S}$, the radius of the ISCO increases. The hatched region denotes the interval of radii over which an orbit is stable on the equatorial plane but unstable perpendicularly.

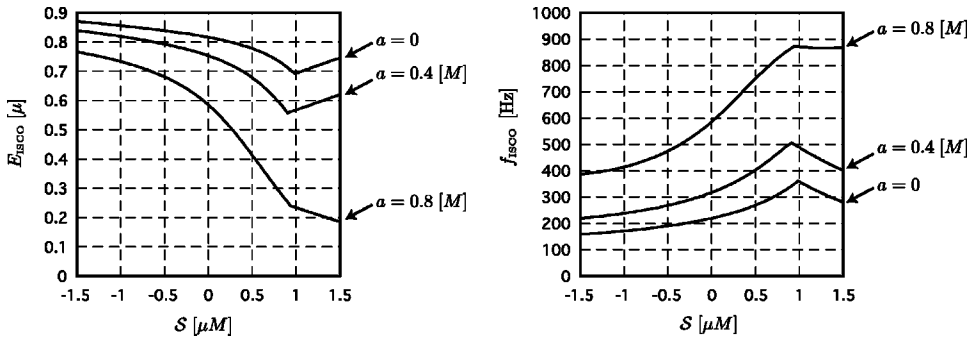

FIG. 4. (a) The particle energy E of the ISCO. (b) The orbital frequency of the ISCO for which the mass of the black hole is assumed to be $10M_{\odot}$.

result for the $a=0$ case is shown in Fig. 5. The name of classified types in this figure are same as those of the ''effective potential'' in [11] in which the circular orbit shows the same stability type as the present analysis. Since the region of $J_z \geqslant 3.5\mu M$ and $\mathcal{S} \geqslant 0$ coincides with Fig. 3 in [11], we believe that the present classification is the same as the previous one by use of the ''effective potential.'' Figure 6 is the classification for the Kerr background spacetime. We expected that the parameter region for the type(U2) potential for Kerr background spacetime would be larger than that for Schwarzschild spacetime because of the lower symmetry and the existence of the spin-spin interaction. However, as we have seen in Fig. 2, the parameter region is not enlarged abruptly as a increases. Rather, for large a, this region gets narrow.

Since our system is not integrable as shown in [11], it may be worth mentioning about a chaotic motion of a spinning test particle in Kerr background spacetime. In our previous paper, we estimated the Lyapunov exponent of a motion of a spinning test particle in the Schwarzschild spacetime. We found that the timescale for which the chaotic motion becomes much longer than the dynamical one. Since we are interested in analysis of a compact binary system, we will not discuss unbounded orbits such as in the type(U1) and type(U2) potentials in this paper, although it may also be interesting to analyze those. Then we may conclude that a particle motion can be chaotic and such a chaotic behavior could affect a template of gravitational waves emitted from a binary system only in the case of type(B2) potential.

As we see from Fig. 6, the type(B2) region becomes larger as a increases. Then, we expect that a particle motion in Kerr spacetime may become more chaotic than that in Schwarzschild spacetime. This is consistent with the fact that Kerr spacetime possesses lower symmetry than Schwarzschild spacetime and therefore the number of the constants of motion is smaller than that in the Schwarzschild case. As for an example, we show in Fig. 7 the Poincaré map of four orbits for the $a=0.8M$ case constructed with the same rule as in [11]. These four orbits have different initial conditions but same parameters of the motion, i.e., $J_z=2.8\mu M$ and $\mathcal{S}=0.4\mu M$, which are in the type(B2) region. We can see that the torus structures are broken and the motions of these orbits are chaotic. For the Schwarzschild case, the lowest value of the spin for which chaos occurs is about $0.6\mu M$ (Fig. 7 in [12]). It is much higher than that in the above Kerr case ($\mathcal{S}=0.4\mu m$). This result supports our expectation that a particle motion in Kerr spacetime is more chaotic than that in Schwarzschild case [14].

In this paper, we have analyzed the stability of a circular orbit of a spinning test particle in a Kerr background spacetime using the linear perturbation method. The circular orbit can be unstable not only in the r direction but also in the θ direction due to the spin. This instability occurs when the parameters are within the shaded regions of Fig. 2. In Fig. 8,

TABLE I. The stability of a spinning test particle on the equatorial plane.

	Inner extremal point		Outer extremal point	
	r direction	θ direction	r direction	θ direction
Type(B1)	Unstable	Stable	Stable	Stable
Type(B2)	Unstable	Unstable	Stable	Stable
Type(U1)		No extremal point		
Type(U2)	Unstable	Unstable	Stable	Unstable

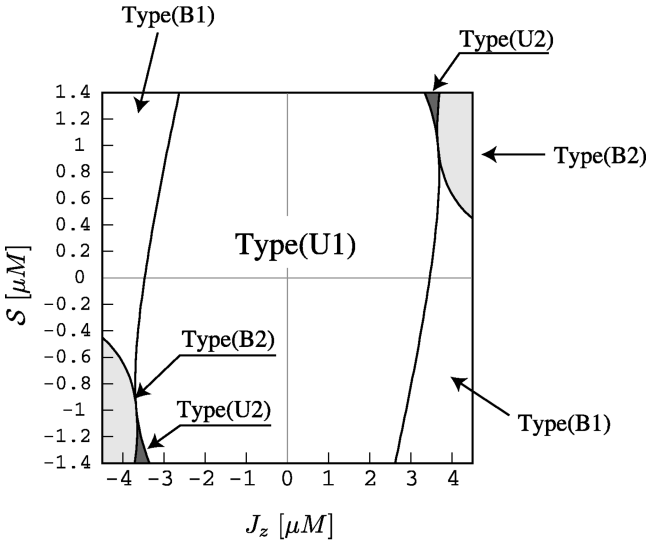

FIG. 5. The classification of the ''effective potential'' of the particle for the $a=0$ case in the J_z-$\mathcal{S}$ plane. The region $J_z > 3.5\mu M$ and $\mathcal{S}>0$ is the same as Fig. 3 in [12].

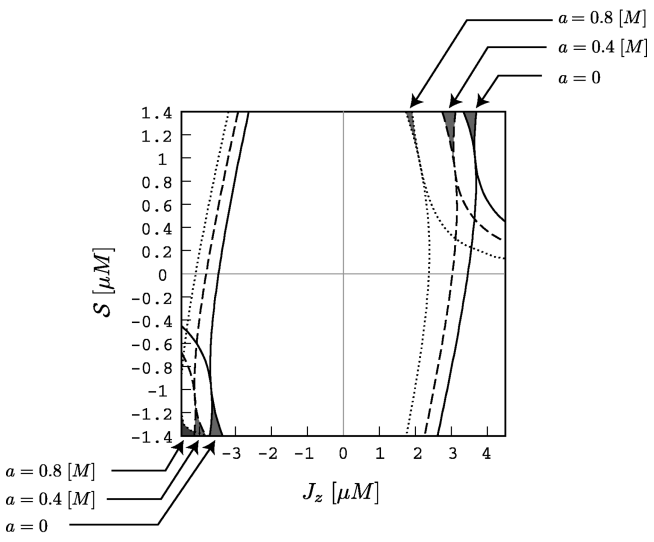

FIG. 6. The classification of the effective potential of the particle on the equatorial plane for a Kerr black hole.

a typical unstable orbit with these parameters and its fate are shown. We have chosen the parameters for the initially circular orbit of the particle as $\mathcal{S}=1\mu M$, $E=0.86199950863\mu$, $J_z=3.06620962243\mu M$, $r_0=3.05M$ and $\theta=\pi/2$. The Kerr parameter is $a=0.4M$. For a perturbation, the direction of the spin is set to be slightly different from the perpendicular to the equatorial plane, i.e. $\delta S^3=3.672835\times10^{-5}\mu M$. Because this circular orbit is unstable in the θ direction, the particle leaves the equatorial plane and falls into the black hole eventually. Therefore this type of instability may change the radius of the ISCO. In Fig. 3, the dependence of the radius of the ISCO upon the magnitude of the spin is shown. In Fig. 4, the energy of the particle on the ISCO and the orbital frequency of the ISCO are also depicted.

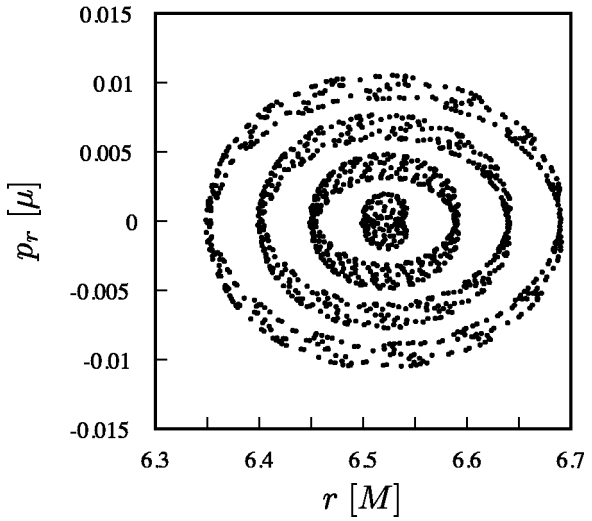

FIG. 7. The Poincaré map for the orbit in a Kerr spacetime, $a=0.8M$, with parameters which belong to the type(B2). All orbits have $J_z=2.8\mu M$, $\mathcal{S}=0.4\mu M$ and $E=0.9275\mu$. We set $p^r=0$ initially. And the initial position is $r_0=6.5$, 6.592, 6.628 and $6.68M$. We find that the motion is chaotic.

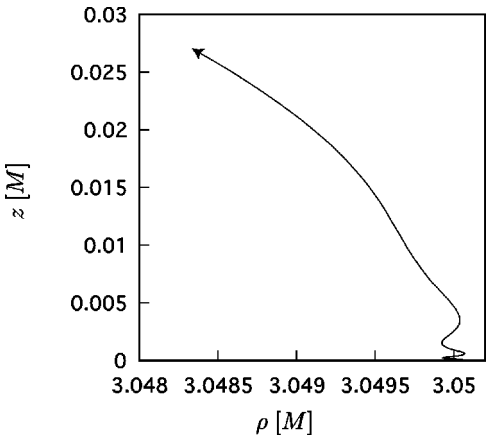

FIG. 8. The orbit of a spinning particle in the type(U2) potential in Kerr background spacetime with $a=0.4M$. The particle is at the minimum point of the ''effective potential'' in the r direction on the equatorial plane and the direction of the spin vector is slightly deviated from the direction perpendicular to the equatorial plane initially. The parameters of the orbit are $J_z=3.06620962243\mu M$, $E=0.86199950863\mu$, $\mathcal{S}=1.0\mu M$ and $r_0=3.05M$. The initial perturbation is $\delta S^3=3.672835\times10^{-5}\mu M$.

If this new type of instability occurs in a real astrophysical system such as a binary system, it changes the radius of the ISCO. This is very important for observation, especially, gravitational astronomy as mentioned in the Introduction. So, we may restrict the parameters of the system, for example the lower limit of the spin, from the observation of gravitational waves. And the chaos is also an important factor for gravitational wave astronomy, because if chaos occurs in the system, it must affect the gravitational wave emitted from the system. However, the test particle model should not be adopted as a model of the last stage of a binary system. In fact, in our analysis, the radius of the ISCO gets very small. For such small distances to the horizon, instabilities due to other effects mentioned in the Introduction must be taken into account. Therefore, we need further investigation to check the importance of this type of instability in a more realistic binary system.

ACKNOWLEDGMENTS

We would like to thank Paul Haines for his critical reading of our paper. This work was supported partially by the Grant-in-Aid for Scientific Research Fund of the Ministry of Education, Science and Culture (Specially Promoted Research No. 08102010), by a JSPS Grant-in-Aid (No. 095790), and by the Waseda University Grant for Special Research Projects.

APPENDIX A: THE PERTURBATION MATRIX AND ITS EIGENVALUE EQUATION

Here, we present the explicit form of the perturbation matrix in Eq. (3.15) and its non-vanishing components:

$$\begin{pmatrix} A^i{}_j & B^i{}_j & C^i{}_j \\ D^i{}_j & E^i{}_j & F^i{}_j \\ G^i{}_j & H^i{}_j & I^i{}_j \end{pmatrix} = \begin{pmatrix} 0 & A^0{}_1 & 0 & 0 & B^0{}_0 & 0 & 0 & 0 & 0 & 0 & C^0{}_2 & 0 \\ 0 & 0 & 0 & 0 & 0 & B^1{}_1 & 0 & 0 & 0 & 0 & 0 & 0 \\ 0 & 0 & 0 & 0 & 0 & 0 & B^2{}_2 & 0 & C^2{}_0 & 0 & 0 & C^2{}_3 \\ 0 & A^3{}_1 & 0 & 0 & 0 & 0 & 0 & B^3{}_3 & 0 & 0 & C^3{}_2 & 0 \\ 0 & 0 & 0 & 0 & 0 & E^0{}_1 & 0 & 0 & 0 & 0 & 0 & 0 \\ 0 & D^1{}_1 & 0 & 0 & E^1{}_0 & 0 & 0 & E^1{}_3 & 0 & 0 & F^1{}_2 & 0 \\ 0 & 0 & D^2{}_2 & 0 & 0 & 0 & 0 & 0 & 0 & F^2{}_1 & 0 & 0 \\ 0 & 0 & 0 & 0 & 0 & E^3{}_1 & 0 & 0 & 0 & 0 & 0 & 0 \\ 0 & 0 & G^0{}_2 & 0 & 0 & 0 & 0 & 0 & 0 & I^0{}_1 & 0 & 0 \\ 0 & 0 & 0 & 0 & 0 & 0 & H^1{}_2 & 0 & I^1{}_0 & 0 & 0 & I^1{}_3 \\ 0 & 0 & 0 & 0 & 0 & 0 & 0 & 0 & 0 & 0 & 0 & 0 \\ 0 & 0 & G^3{}_2 & 0 & 0 & 0 & 0 & 0 & 0 & I^3{}_1 & 0 & 0 \end{pmatrix}, \tag{A1}$$

where

$$A^0{}_1 = \frac{3M\mathcal{S}^2\sqrt{\Delta}}{\mu^3 r_0^5} p^0_{(0)} - \left(\frac{\sqrt{\Delta}}{r}\right)'\Big|_{r=r_0} v^0_{(0)},$$

$$A^3{}_1 = -\frac{2a}{r_0^2} v^0_{(0)} - \frac{\sqrt{\Delta}}{r_0^2} v^3_{(0)} - \frac{6M\mathcal{S}^2\sqrt{\Delta}}{\mu^3 r_0^5} p^3_{(0)},$$

$$B^0{}_0 = \frac{1}{\mu}\left(1 - \frac{M\mathcal{S}^2}{\mu^2 r_0^3}\right),$$

$$B^1{}_1 = \frac{1}{\mu}\left(1 - \frac{M\mathcal{S}^2}{\mu^2 r_0^3}\right),$$

$$B^2{}_2 = \frac{1}{\mu},$$

$$B^3{}_3 = \frac{1}{\mu}\left(1 + \frac{2M\mathcal{S}^2}{\mu^2 r_0^3}\right),$$

$$C^0{}_2 = \frac{2M\mathcal{S}}{\mu^3 r_0^3} p^0_{(0)},$$

$$C^2{}_0 = \frac{M\mathcal{S}}{\mu^3 r_0^3} p^0_{(0)},$$

$$C^2{}_3 = \frac{2M\mathcal{S}}{\mu^3 r_0^3} p^3_{(0)},$$

$$C^3{}_2 = -\frac{4M\mathcal{S}}{\mu^3 r_0^3} p^3_{(0)},$$

$$D^1{}_1 = -\frac{3M\mathcal{S}^2\sqrt{\Delta}}{\mu^3 r_0^5}\left(\frac{\sqrt{\Delta}}{r}\right)'\Big|_{r=r_0} (p^0_{(0)})^2 - \frac{3Ma\mathcal{S}^2\sqrt{\Delta}}{\mu^3 r_0^7} p^0_{(0)} p^3_{(0)} - \frac{6M\mathcal{S}^2\Delta}{\mu^3 r_0^7} (p^3_{(0)})^2 - \frac{\sqrt{\Delta}}{r_0}\left(\frac{\sqrt{\Delta}}{r^2}\right)''\Big|_{r=r_0} v^0_{(0)} p^0_{(0)} + \frac{\sqrt{\Delta}}{r_0}\left(\frac{\sqrt{\Delta}}{r^2}\right)'\Big|_{r=r_0} v^3_{(0)} p^3_{(0)} - \frac{\sqrt{\Delta}}{\mu r_0^5}[(2a\mu r_0 + 3M\mathcal{S}) v^3_{(0)} p^0_{(0)} + 2(a\mu r_0 + 3M\mathcal{S}) v^0_{(0)} p^3_{(0)}],$$

$$D^2{}_2 = -\frac{a}{\mu r_0^5}(a\mu r_0 + 3M\mathcal{S}) v^0_{(0)} p^0_{(0)} - \frac{1}{\mu r_0^5}[\mu r_0 (r_0^2 + a^2) + 6M\mathcal{S}] v^3_{(0)} p^3_{(0)} - \frac{a\sqrt{\Delta}}{r_0^4}(v^3_{(0)} p^0_{(0)} + v^0_{(0)} p^3_{(0)}),$$

$$E^0{}_1 = \frac{a\mu + 2M\mathcal{S}}{\mu^2 r_0^3}\left(1 - \frac{M\mathcal{S}^2}{\mu^2 r_0^3}\right) p^3_{(0)} - \left(\frac{\sqrt{\Delta}}{r}\right)'\Big|_{r=r_0} v^0_{(0)} + \frac{a\mu + M\mathcal{S}}{\mu r_0^3} v^3_{(0)},$$

$$E^1{}_0 = \frac{a\mu + 2M\mathcal{S}}{\mu^2 r_0^3}\left(1 - \frac{M\mathcal{S}^2}{\mu^2 r_0^3}\right) p^3_{(0)}$$

$$-2\left(\frac{\sqrt{\Delta}}{r}\right)'\Big|_{r=r_0} v^0_{(0)} + \frac{a\mu+M\mathcal{S}}{\mu r_0^3} v^3_{(0)},$$

$$E^1{}_3 = \frac{a\mu+M\mathcal{S}}{\mu^2 r_0^3}\left(1+\frac{2M\mathcal{S}^2}{\mu^2 r_0^3}\right)p^0_{(0)} + \frac{a\mu+2M\mathcal{S}}{\mu r_0^3} v^0_{(0)} + \frac{2\sqrt{\Delta}}{r_0^2} v^3_{(0)},$$

$$E^3{}_1 = -\frac{\sqrt{\Delta}}{r_0^2} v^3_{(0)},$$

$$F^1{}_2 = -\frac{2M\mathcal{S}}{\mu^3 r_0^3}\left(\frac{\sqrt{\Delta}}{r}\right)'\Big|_{r=r_0} (p^0_{(0)})^2 - \frac{2Ma\mathcal{S}}{\mu^3 r_0^5} p^3_{(0)} p^0_{(0)} - \frac{4M\mathcal{S}\sqrt{\Delta}}{\mu^3 r_0^5}(p^3_{(0)})^2 - \frac{M}{\mu r_0^3}(v^3_{(0)} p^0_{(0)} + 2 v^0_{(0)} p^3_{(0)}),$$

$$G^0{}_2 = \frac{3Ma\mathcal{S}^2}{\mu^3 r_0^5}(v^0_{(0)} p^0_{(0)} + v^3_{(0)} p^3_{(0)}) p^0_{(0)} + \frac{a^2\mathcal{S}}{r_0^4} v^0_{(0)} + \frac{a\mathcal{S}\sqrt{\Delta}}{r_0^4} v^3_{(0)},$$

$$G^3{}_2 = \frac{3Ma\mathcal{S}^2}{\mu^3 r_0^5}(v^0_{(0)} p^0_{(0)} + 2 v^3_{(0)} p^3_{(0)}) p^3_{(0)} - \frac{a\mathcal{S}\sqrt{\Delta}}{r_0^4} v^0_{(0)} - \frac{\mathcal{S}(r_0^2+a^2)}{r_0^4} v^3_{(0)},$$

$$H^1{}_2 = -\frac{\mathcal{S}\sqrt{\Delta}}{\mu r_0^2},$$

$$I^0{}_1 = \frac{3M\mathcal{S}}{\mu^3 r_0^3}(v^3_{(0)} p^0_{(0)} + v^0_{(0)} p^3_{(0)}) p^0_{(0)} - \left(\frac{\sqrt{\Delta}}{r}\right)'\Big|_{r=r_0} v^0_{(0)} + \frac{a}{r_0^2} v^3_{(0)},$$

$$I^1{}_0 = -\frac{M\mathcal{S}^2\sqrt{\Delta}}{\mu^3 r_0^5} p^0_{(0)} - \left(\frac{\sqrt{\Delta}}{r}\right)'\Big|_{r=r_0} v^0_{(0)} + \frac{a}{r_0^2} v^3_{(0)},$$

$$I^1{}_3 = -\frac{2M\mathcal{S}^2\sqrt{\Delta}}{\mu^3 r_0^5} p^3_{(0)} + \frac{a}{r_0^2} v^0_{(0)} + \frac{\sqrt{\Delta}}{r_0^2} v^3_{(0)},$$

$$I^3{}_1 = \frac{3M\mathcal{S}}{\mu^3 r_0^3}(v^3_{(0)} p^0_{(0)} + v^0_{(0)} p^3_{(0)}) p^3_{(0)} - \frac{a}{r_0^2} v^0_{(0)} - \frac{\sqrt{\Delta}}{r_0^2} v^3_{(0)}.$$

A prime denotes d/dr. It is easily shown that the eigenequation of the matrix (A1) can be decomposed as follows:

$$\lambda^3 \begin{vmatrix} -\lambda & 0 & 0 & B^1{}_1 \\ 0 & -\lambda & 0 & E^0{}_1 \\ 0 & 0 & -\lambda & E^3{}_1 \\ D^1{}_1 & E^1{}_0 & E^1{}_3 & -\lambda \end{vmatrix} \times \begin{vmatrix} -\lambda & 0 & 0 & D^2{}_2 & F^2{}_1 \\ 0 & -\lambda & 0 & G^0{}_2 & I^0{}_1 \\ 0 & 0 & -\lambda & G^3{}_2 & I^3{}_1 \\ B^2{}_2 & C^2{}_0 & C^2{}_3 & -\lambda & 0 \\ H^1{}_2 & I^1{}_0 & I^1{}_3 & 0 & -\lambda \end{vmatrix} = 0. \quad \text{(A2)}$$

Three zero eigenvalues come from two zero columns and a zero line in the matrix, which are related to the facts that t and ϕ are the cyclic coordinates of the system and that the magnitude of the spin is conserved, respectively. The second part consists of the components related to $\delta x^1, \delta p^0, \delta p^3$ and δp^1. Because of the conservation of the energy and the angular momentum of the particle, two eigenvalues of this part are zero. The remaining two eigenvalues describe the stability in the r direction. The components of the last part are related to δp^2, δS^0, δS^3, δx^2 and δS^1. The eigenequation of this part, except for one zero eigenvalue which comes from the condition (2.13), turns out to be a quadratic equation of λ^2 and determines the stability in the θ direction. Finally, we find the eigenvalue equation as,

$$\lambda^6(\lambda^2 - \Lambda_r)(\lambda^4 - \Lambda_{\theta 1}\lambda^2 + \Lambda_{\theta 2}) = 0, \quad \text{(A3)}$$

where

$$\Lambda_r = (B^1{}_1 D^1{}_1 + E^0{}_1 E^1{}_0 + E^1{}_3 E^3{}_1), \quad \text{(A4)}$$

$$\Lambda_{\theta 1} = (B^2{}_2 D^2{}_2 + C^2{}_0 G^0{}_2 + C^2{}_3 G^3{}_2 + F^2{}_1 H^1{}_2 + I^0{}_1 I^1{}_0 + I^1{}_3 I^3{}_1), \quad \text{(A5)}$$

$$\Lambda_{\theta 2} = (C^2{}_0 F^2{}_1 G^0{}_2 H^1{}_2 + C^2{}_3 F^2{}_1 G^3{}_2 H^1{}_2 - C^2{}_0 D^2{}_2 H^1{}_2 I^0{}_1 - B^2{}_2 F^2{}_1 G^0{}_2 I^1{}_0 + B^2{}_2 D^2{}_2 I^0{}_1 I^1{}_0 + C^2{}_3 G^3{}_2 I^0{}_1 I^1{}_0 - B^2{}_2 F^2{}_1 G^3{}_2 I^1{}_3 - C^2{}_0 G^3{}_2 I^0{}_1 I^1{}_3 - C^2{}_3 D^2{}_2 H^1{}_2 I^3{}_1 - C^2{}_3 G^0{}_2 I^1{}_0 I^3{}_1 + B^2{}_2 D^2{}_2 I^1{}_3 I^3{}_1 + C^2{}_0 G^0{}_2 I^1{}_3 I^3{}_1). \quad \text{(A6)}$$

To analyze the stability of a circular orbit, we have to know Λ_r for the stability in the r direction, while $\Lambda_{\theta 1}$ and $\Lambda_{\theta 2}$ for that in the θ direction.

[1] A. Abromovici, W. E. Althouse, R. W. P. Drever, Y. Gürsel, S. Kawamura, F. J. Raab, D. Shoemaker, L. Sievers, R. E. Spero, K. S. Thorne, R. E. Vogt, R. Weiss, S. E. Whitcomb, and M. E. Zucker, Science **256**, 325 (1992).

[2] C. Cutler, T. A. Apostolatos, L. Bildsten, L. S. Finn, E. E. Franagan, D. Kennefick, D. M. Markovic, A. Ori, E. Poisson, G. J. Sussman, and K. S. Thorne, Phys. Rev. Lett. **70**, 2984 (1993).

[3] For a review, see, e.g., T. Damour, in *300 Years of Gravitation*, edited by S. W. Hawking and W. Israel (Cambridge University Press, Cambridge, England, 1987), p. 128.

[4] L. E. Kidder, Phys. Rev. D **52**, 821 (1995); T. A. Apostolatos, C. Cutler, G. J. Sussman, and K. S. Thorne, *ibid.* **49**, 6274 (1994); T. A. Apostolatos, Class. Quantum Grav. **13**, 799 (1996).

[5] A. Papapetrou, Proc. R. Soc. London **A209**, 248 (1951).

[6] W. G. Dixon, Proc. R. Soc. London **A314**, 499 (1970); **A319**, 509 (1970); Gen. Relativ. Gravit. **4**, 193 (1973); Philos. Trans. R. Soc. London **A277**, 59 (1974); in *Isolated Gravitating Systems in General Relativity*, edited by J. Ehlers (North-Holland, Amsterdam, 1979), p. 156.

[7] I. Bailey and W. Israel, Ann. Phys. (N.Y.) **130**, 188 (1980).

[8] E. Corinaldesi and A. Papapetrou, Proc. R. Soc. London **A209**, 259 (1951).

[9] S. N. Rasband, Phys. Rev. Lett. **30**, 111 (1973); K. P. Tod and F. de Felice, Nuovo Cimento B **34**, 365 (1976); R. Hojman and S. Hojman, Phys. Rev. D **15**, 2724 (1977); M. A. Abramowicz and M. Calvani, Mon. Not. R. Astron. Soc. **189**, 621 (1979); R. Wald, Ann. Phys. (N.Y.) **83**, 548 (1974); R. Wald, Phys. Rev. D **6**, 406 (1972).

[10] Y. Mino, M. Shibata, and T. Tanaka, Phys. Rev. D **53**, 622 (1996); T. Tanaka, Y. Mino, M. Sasaki, and M. Shibata, *ibid.* **54**, 3762 (1996); M. Saijo, K. Maeda, M. Shibata, and Y. Mino (in preparation).

[11] S. Suzuki and K. Maeda, Phys. Rev. D **55**, 4848 (1997).

[12] D. Lai, F. A. Rasio, and S. L. Shapiro, Astrophys. J., Suppl. Ser. **88**, 205 (1993); D. Lai, F. A. Rasio, and S. L. Shapiro, Astrophys. J. **420**, 811 (1994); Astrophys. J. Lett. **406**, L63 (1993); D. Lai and A. G. Wiseman, Phys. Rev. D **54**, 3958 (1996).

[13] C. W. Misner, K. S. Thorne, and J. A. Wheeler, *Gravitation* (W. H. Freeman and Company, New York, 1973).

[14] A detailed analysis for chaos in Kerr background spacetime will be given elsewhere.